Shear instabilities in arrested salt-wedge flows

Noboru Yonemitsu [a], Gordon E. Swaters [b], Nallamuthu Rajaratnam [c],
Gregory A. Lawrence [a, *]

[a] *Environmental Fluid Mechanics, Department of Civil Engineering, University of British Columbia,
Vancouver, B.C. V6T 1Z4, Canada*
[b] *Institute of Applied Mathematics, Department of Mathematics, University of Alberta, Edmonton,
Alta. T6G 2G1, Canada*
[c] *Department of Civil Engineering, University of Alberta, Edmonton, Alta. T6G 2G7, Canada*

Abstract

'One-sidedness' in arrested salt-wedge flows is investigated with theoretical models based upon two-layer approximations. These models include the effects of rigid bottom boundaries and the effects of density interface displacement with respect to the centre of the shear layer. The results indicate that inclusion of both interface displacement and rigid boundaries in the model greatly contribute to the 'one-sidedness' phenomenon and influence the wave characteristics, especially their stability criteria. Data from laboratory experiments agreed well with the results produced by these models.

1. Introduction

'One-sidedness' (Keulegan, 1966; Browand and Winant, 1973) is a classic problem in the study of mixing processes in two-layered stratified flows. This phenomenon, which is associated with the breaking of the density interface, tends to be confined to the high-speed side of the flow, and is commonly observed in arrested salt wedges. Fig. 1 shows a schematic diagram of a salt wedge. The longitudinal sub-divisions were defined by Sargent and Jirka (1987) using the force balances. Two different kinds of interfacial waves (positive and negative waves) are observed; they propagate in opposite directions. The positive waves cusp upwards and occasionally break into the upper layer. They appear near the tip region and
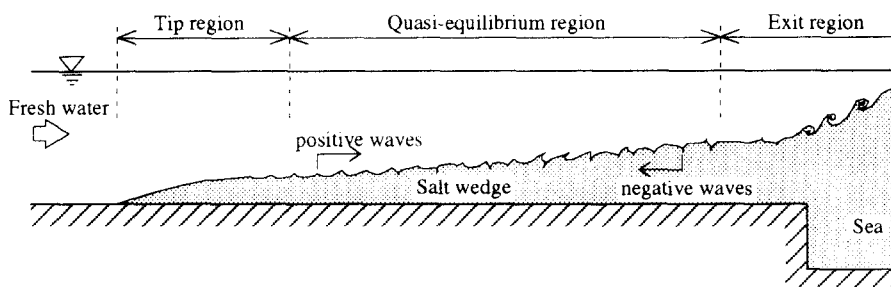
---

* Corresponding author.

Fig. 1. Schematic structure of a salt-wedge flow with three longitudinal subdivisions (based upon its force balance) and its typical interfacial waves.

propagate in the downstream direction. In contrast, the negative waves cusp towards the lower layer, and are commonly observed near the exit region. This is the one-sidedness phenomenon in salt-wedge flows. Although many attempts have been made to interpret this phenomenon as shear instability, they fail to clarify its mechanism, mainly because of the lack of appropriate models.

One of the problems associated with analysis of this type of flow is the modelling of the velocity profile. Most models employ time-averaged velocity profiles which are generally anti-symmetric to the density interface. Interfacial waves, however, are known to be intermittent and consequently must be considered as events dependent on the instantaneous velocity distribution. Our observations show that instantaneous velocity profiles often have a displacement between the centre of the shear layer and the density interface, and the stability characteristics of such flows are known to be different from those of anti-symmetric cases (Lawrence et al., 1991). Another modelling problem is that most of the stability analyses have neglected the existence of rigid boundaries for simplicity. It is obvious that the bottom boundary effects on salt-wedge flows are not negligible.

The effects of rigid boundaries were first investigated by Howard (1963), and Hazel (1972) for inviscid flows. This study was followed by those of Davis and Peltier (1976, 1977), Lalas and Einaudi (1976), Lindzen and Rosenthal (1976), and Fua and Einaudi (1984), to solve atmospheric boundary layer problems. Hazel showed, in one of his models (continuous velocity and density profiles), that flows were stable for the range of non-dimensionalized lower layer thickness $0 < ZR < 1.195–1.205$, despite some numerical instability problems. These models are, however, designed for atmospheric boundary layers, and hence their results, owing to their density profiles, are not directly applicable to the salt-wedge flows.

In this paper, we report first on the experiments we performed to obtain detailed information on the flow field, which is often three-dimensional. These experiments determined the appropriate functions for modelling the velocity profile for two-layered stratified flow; we then calculated the stability characteristics assuming the existence of rigid boundaries, interface displacements and viscosity.

2. Experiments

The aim of our experiments was to identify the relationships among three-dimensional flow structures, velocity profiles, interfacial displacements, lower layer thickness, and associated interfacial waves. Sixty-three salt wedge experiments were conducted in the flume shown in Fig. 2. Flow visualization was employed to obtain the flow structure and wave characteristics, and laser Doppler anemometer (LDA) and dye injection (see Yoshida, 1980) were used to measure the velocity profiles. Density interface position and thickness were measured by using conductivity probes, and throughout the experiments the interface thickness was found to be less than one-tenth of the shear layer thickness. This result justifies the use of two-layered models.

The results of the flow visualization can be summarized as shown in Fig. 3. It was impossible to eliminate side and bottom boundary effects from our experiments, and consequently the flows in this channel exhibited a three-dimensional structure. The secondary flows, induced by several pairs of stream-wise vortices in the upper layer, cause a wave-like transverse variation in the longitudinal velocity. For our convenience, we shall introduce transverse subdivisions such as the high-speed region (HSR) and the low-speed region (LSR), according to the longitudinal velocity in the upper layer. In the HSR, the lower layer tends to be thin because of higher shear stress, i.e. higher entrainment at the density interface. In this region, the volume of entrained salt water is much larger than that of the back flow in the lower layer; therefore mass-balance is not valid in a two-dimensional sense. Similarly, in the LSR the velocity profile indicates less interfacial shear stress, which causes less entrainment than back flow. By summing the fluxes of the HSR and the LSR, the salt wedge maintains its stationary position, i.e. mass is conserved. Therefore, transverse subdivisions must be considered when the experimental data are analysed and interpreted.

Flow visualization also revealed the existence of waves travelling in different directions with the mean flow. These waves are reminiscent of Holmboe's (1962)
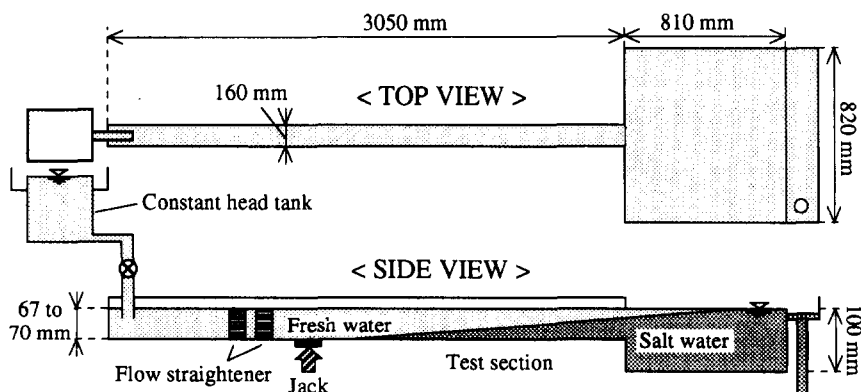
Fig. 2. Experimental apparatus. The bed slope of the channel can be adjusted with the hydraulic jack. The conductivity probes, wave sensors and LDA optics are located in the test section.
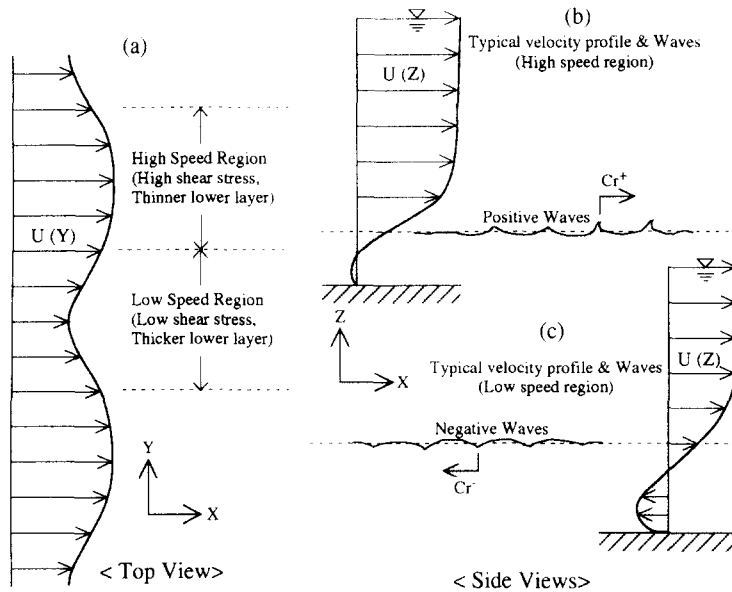
Fig. 3. Three-dimensional flow structure, velocity profiles and interfacial waves created mainly by the secondary flow (steam-wise vortex pairs) in an experimental channel. X, Y, Z are Cartesian coordinates corresponding to the longitudinal, lateral and vertical direction, respectively. U in this figure is velocity in the X direction. (Note that the inflection point of the velocity profiles is located above the density interface in the high speed region (b), and below in the low speed region (c).)

instability, which consists of positive and negative instabilities of equal growth rates and equal but opposite phase speeds. Similar disturbances have also been observed by Tsubaki et al. (1969), Murota and Hirata (1978) and Yoshida (1980). Our study differs from previous work in that the positive and the negative waves appear in different locations on the salt wedge. This is the one-sidedness phenomenon in salt-wedge flows. The positive waves, which are induced by vortex tubes just above the density interface (Lawrence et al., 1991), cusp upwards. They are observed most of the time in the HSR near the tip region, and propagate in the downstream direction. The negative waves, which cusp towards the lower layer, can be found in the LSR near the exit region, and propagate slowly upstream. Interaction between these two waves occurs somewhere in the quasi-equilibrium region.

Velocity profiles measured in both the HSR and the LSR are shown in Fig. 4. In Fig. 4(a), length and velocity scales are non-dimensionalized based upon the definition given in Fig. 4(b), and the displacement ϵ is removed. The results in Fig. 4(a) indicate that velocity profiles can be approximated by the tanh function very well, and therefore the non-dimensionalization by the length scale L and velocity scale U is justified. The non-dimensional parameters are defined as

$$\alpha = \frac{2\pi L}{\lambda}, \qquad \gamma = \frac{\rho_1}{\rho_2}, \qquad Ri = \frac{(1-\gamma)gL}{U^2}, \qquad Re = \frac{UL}{\nu} \qquad (1)$$
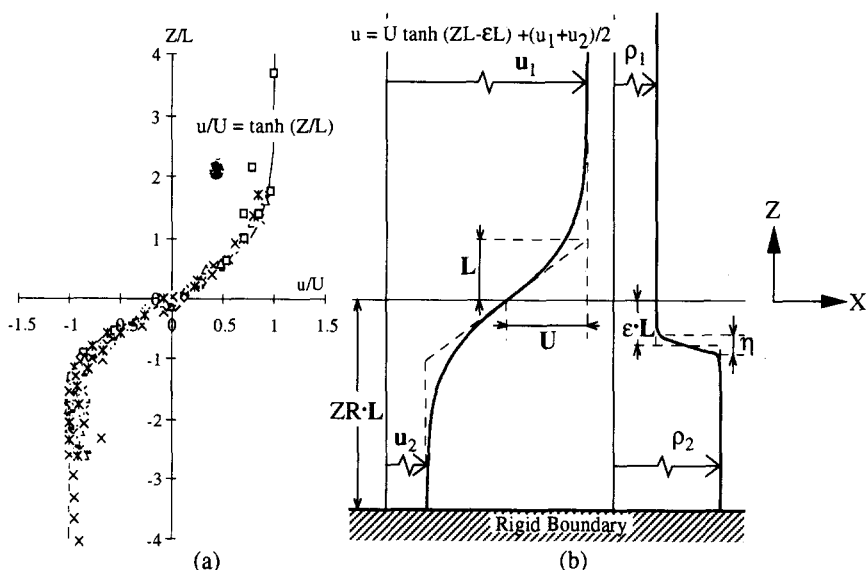
Fig. 4. (a) Observed velocity profiles and (b) definition of velocity and length scale. The interfacial displacement ϵ is removed in (a). Notations are: x, z, Cartesian coordinate system located at the density interface, with u_1, u_2, velocity in upper and lower layer; ρ_1, ρ_2, density in upper and lower layer; ZR, the lower layer thickness; L, U, the characteristic length and velocity scales; ϵ, the displacement of the centre of shear layer and density interface (non-dimensionalized); η, the density interface thickness.

where Ri is the overall Richardson number, Re is the Reynolds number, α is the wavenumber, λ is the wavelength, ν is the kinematic viscosity of water and g is gravitational acceleration.

Fig. 5 shows observations of interface displacement ϵ with Ri and the lower layer thickness ZR. These plots imply that (1) most of the positive waves occur where the values of ϵ are positive, (2) the negative waves have very small Ri and
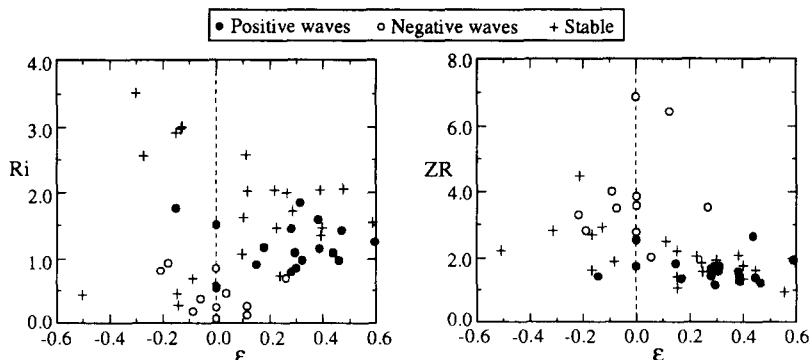

Fig. 5. Interfacial displacement ϵ vs. Richardson number Ri and lower layer thickness ZR.

relatively large ZR, and (3) there is no specific value of ϵ for the negative waves. It was also found that the distance between upper boundary (free surface) and density interface is always greater than 5.0, and therefore it is considered large enough that the free surface has no effects on interfacial phenomena (see the results of numerical analysis by Hazel (1972), Nishida and Yoshida (1987) and Yonemitsu (1991)). It is especially interesting that some positive unstable waves have much larger Ri than 1.4, which is predicted as the stability boundary by Nishida and Yoshida (1987).

It can be concluded that the interfacial waves on the salt wedge flows must be analysed by appropriate models based upon more realistic velocity profiles and boundary conditions than have been used in existing theories. The following theoretical analysis is therefore designed to evaluate the effects of interfacial displacement and rigid boundaries on the stability characteristics of two-layered stratified flows.

3. Theoretical development

Hino and Hung (1982) analysed the stability characteristics of salt-wedge flows by solving equations for viscous-diffusive systems, with realistic velocity (tanh function for the upper-layer velocity profile and second-order polynomial function for the lower-layer velocity profile) and density profiles ($\rho(z) = \exp[-\gamma \tan(Rz)/R]$ where R is the ratio of shear layer to density interface thickness), and having a rigid bottom boundary. Their analysis failed, however, to provide any unstable solutions, and it could not distinguish the effects of viscosity, diffusivity, rigid boundary and velocity profiles, owing to their complicated models.

In the model described here we employed relatively simple and realistic velocity (tanh function) and density (two-layer approximation) profiles to avoid any further complexity, then evaluated the effects of the rigid boundary and the interfacial displacement separately. Two models are examined by the linear stability theory. One of them was designed to test the effects of a rigid boundary and the other to investigate the interfacial displacement. Their velocity and density profiles are shown in Figs. 6 and 7. The governing equation is derived by applying infinitesimally small monochromatic perturbations to the two-dimensional, incompressible flow system. A two-layer approximation of the density distribution is made for simplification. The stream function of the perturbation is defined as $\Phi(z)\exp[i\alpha(x - ct)]$, where $\Phi(z)$ is the complex amplitude. This stream function is governed by the Orr–Sommerfeld (O–S) equation:

$$[u(z) - c]\left(\frac{d^2}{dz^2} - \alpha^2\right)\Phi(z) - \frac{d^2u(z)}{dz^2}\Phi(z)$$

$$= \frac{1}{i\alpha\mathrm{Re}}\left(\frac{d^4}{dz^4} - 2\alpha^2\frac{d^2}{dz^2} + \alpha^4\right)\Phi(z) \tag{2}$$
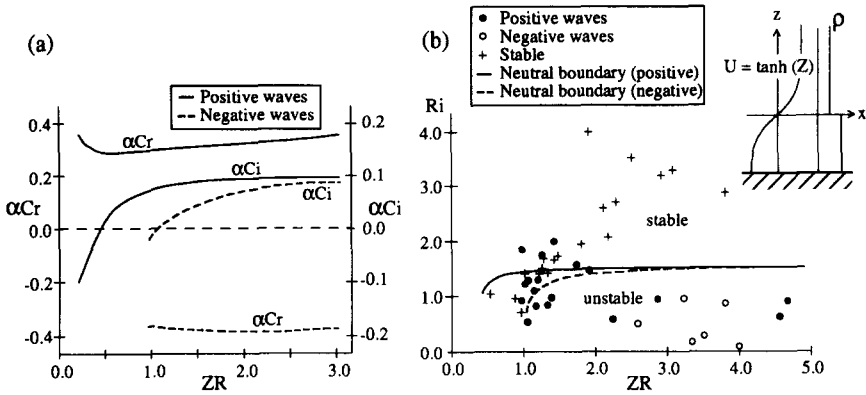
Fig. 6. ZR effects on the stability of positive and negative waves. (a) Growth rate αCi and phase velocity Cr of Re = 100, Ri = 0.4, α = 0.8 solutions, (b) comparison of the nuetral boundaries (αCi = 0.0) for Re = 100 and experimental results.

where i is $(-1)^{1/2}$. The lower and upper boundary conditions are given by

$$\Phi(z) = \frac{d\Phi(z)}{dz} = 0 \quad \text{at} \quad z = -ZR, \infty \tag{3}$$

The matching conditions at the density interface, i.e. the continuity of both normal and shear stress, can be written as

$$\Phi_1 = \Phi_2$$

$$\frac{d\Phi_1}{dz} - \frac{du/dz}{u-c}\Phi_1 = \frac{d\Phi_2}{dz} - \frac{du/dz}{u-c}\Phi_2$$

$$\gamma\frac{d^2\Phi_1}{dz^2} - \gamma\left(\frac{d^2u/dz^2}{u-c} - \alpha^2\right)\Phi_1 = \frac{d^2\Phi_2}{dz^2} - \left(\frac{d^2u/dz^2}{u-c} - \alpha^2\right)\Phi_2$$

$$i\gamma\frac{d^3\Phi_1}{dz^3} + \gamma\alpha[\text{Re}(u-c) - 3i\alpha]\frac{d\Phi_1}{dz} - \gamma\alpha\text{Re}\frac{du}{dz}\Phi_1 \tag{4}$$

$$= i\frac{d^3\Phi_2}{dz^3} + \alpha[\text{Re}(u-c) - 3i\alpha]\frac{d\Phi_2}{dz} - \alpha\text{Re}\frac{du}{dz}\Phi_2 - \frac{\alpha\text{ReRi}}{u-c}\Phi_2,$$

at $z = 0$

where subscripts 1 and 2 correspond to the upper and lower layer, respectively. Details have been given by Nishida and Yoshida (1987). The Runge–Kutta–Gill numerical integration and the filtered method (e.g. Betchov and Criminale, 1967; Gersting and Jankowski, 1972) have been employed to solve the system (2)–(4). The eigenvalues c are obtained by the shooting method. The results are plotted along with the experimental data in Figs. 6 and 7. Re = 100 is chosen as a typical value to match the range of experimental data (29.4 < Re < 549.0).

Fig. 6 shows that the presence of a rigid boundary greatly stabilizes the negative instabilities when ZR < 2.0. By contrast, the positive instabilities are only weakly
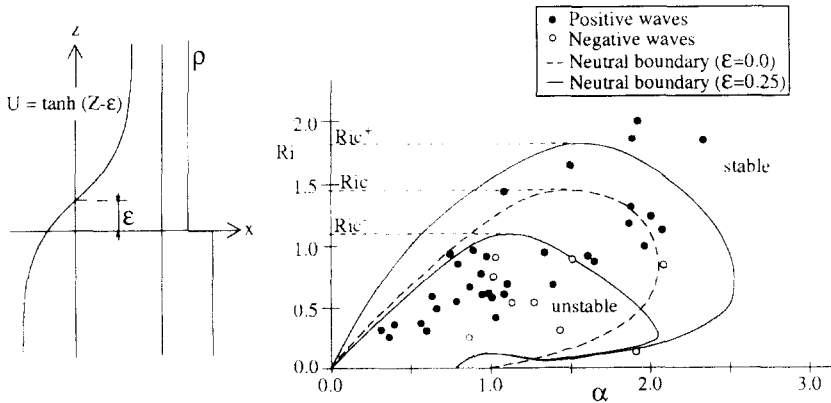
Fig. 7. Stability boundaries with interfacial displacements (Re = 100) and experimental results. Ric^{+} and Ric^{-} correspond to the critical Richardson number for the positive and negative instabilities, respectively.

influenced by variations of ZR. For the positive instabilities, the only noticeable difference between the unbounded case (i.e. $ZR = \infty$) and $ZR < 5.0$ is that the wavenumber of the most unstable waves tends to be smaller (longer wavelength) as ZR decreases. Similar results were found in the inviscid theories (Yonemitsu, 1991). For the case Re = 100, the stability criteria predicted by our analysis for positive and negative waves are $ZR = 0.46$ and 1.10, respectively. This means that no wave can be found for $0 < ZR < 0.46$, only positive waves can exist for $0.46 < ZR < 1.10$, and both positive and negative waves may be observed for $1.10 < ZR$ cases. In salt-wedge flows, the tip region (where ZR is very small) shows no waves; then positive waves appear as the lower layer thickness increases. Further downstream, where ZR is large enough, both positive and negative waves are observed. Therefore these observations are consistent with a theoretical analysis which includes consideration of rigid boundary effects.

Nishida and Yoshida (1987) showed that the critical Richardson number Ric (which is defined as the maximum Richardson number for unstable waves) is relatively insensitive to the variation of the Reynolds number Re (for $20 < Re < 1000$) and remains constant ($Ric \approx 1.4$). The experimental values of Ric for positive waves (Ric^{+}) are, however, larger than our model's prediction as shown in Fig. 6. This problem can be clarified by considering the effects of the interfacial displacement ϵ. In Fig. 7, $\epsilon = 0.0$ and $\epsilon = 0.25$ are chosen as examples. As in the results of Lawrence et al. (1991), the stability boundaries for the positive and negative instabilities bifurcate and stability characteristics change drastically as ϵ increases. Ric^{+} becomes larger as ϵ increases (e.g. $Ric^{+} \approx 2.2$ when $\epsilon = 0.5$) and therefore the relatively large Ric for positive waves from our experiments can be understood as a result of the interfacial displacement. In a somewhat similar way, the negative waves with large wavenumbers can be unstable when interfacial displacement effects are included.

Analyses of both rigid boundary effects and displacement effects indicate that the positive instability always has the greater predicted growth rate for any given Ri. This means that the Holmboe (1962) instability can occur only when $ZR = \infty$ and $\epsilon = 0$. For salt-wedge flows, 'one-sidedness' is therefore the natural state of the wave phenomenon because of the existence of rigid boundaries and interfacial displacement.

4. Conclusions

The 'one-sidedness' phenomenon is explained by a hydrodynamic stability theory including the effects of rigid boundary and interfacial displacement. Our viscous models show the significant details of the salt-wedge flows such as the critical Richardson number (Ric) and unstable wavenumbers. In the case of $Re = 100$, the stability criteria are given as $ZR = 0.46$ for positive waves and $ZR = 1.1$ for negative waves, i.e. $0 < ZR < 0.46$ means no waves, $0.46 < ZR < 1.10$ means only positive waves, and $1.10 < ZR$ means both positive and negative waves can be found. Also, the critical Richardson number is determined as Ric = 1.6 for $\epsilon = 0.25$ and Ric = 2.2 for $\epsilon = 0.5$. Our experimental data verify these theoretical results. Because the characteristics of Holmboe instabilities are very sensitive to the parameters ZR and ϵ, experimental data must be analysed and interpreted carefully. For salt-wedge flows, 'one-sidedness' is the natural state of the wave phenomenon because of the existence of rigid boundaries and interfacial displacement.

Acknowledgements

References

Betchov, R. and Criminale, W.O., 1967. Stability of Parallel Flows. Academic Press, London.

Browand, F.K. and Winant, C.D., 1973. Laboratory observations of shear-layer instability in a stratified fluid. Boundary Layer Meteorol., 5: 67–77.

Davis, P.A. and Peltier, W.R., 1976. Resonant parallel shear instability in the stably stratified planetary boundary layer. J. Atmos. Sci., 33: 1287–1300.

Davis, P.A. and Peltier, W.R., 1977. Effects of dissipation on parallel shear instability near the ground. J. Atmos. Sci., 34: 1868–1884.

Fua, D. and Einaudi, F., 1984. On the effect of dissipation on shear instabilities in the stable atmospheric boundary layer. J. Atmos. Sci., 41: 888–900.

Gersting, J.M. and Jankowski, D.F., 1972. Numerical methods for Orr–Sommerfeld problems. Int. J. Numer. Methods Eng., 4: 195–206.

Hazel, P., 1972. Numerical studies of the stability of inviscid stratified shear flow. J. Fluid Mech., 51: 39–61.

Hino, M. and Hung, N.G., 1982. The stability and interfacial waves of viscous-diffusive stratified two-layer flows. Proceedings of the 26th Japanese Conference on Hydraulics, pp. 513–519 (in Japanese).

Holmboe, J., 1962. On the behavior of symmetric waves in stratified shear layers. Geofys. Publ., 24: 67–113.

Howard, L.N., 1963. Neutral curves and stability boundaries in stratified flow. J. Fluid Mech., 16: 333–342.

Keulegan, G., 1966. The mechanism of an arrested saline wedge. In: A.T. Ippen (Editor), Estuary and Coastline Hydrodynamics. McGraw–Hill, New York, pp. 546–574.

Lalas, D.P. and Einaudi, F., 1976. On the characteristics of gravity waves generated by atmospheric shear layers. J. Atmos. Sci., 33: 1248–1259.

Lawrence, G.A., Browand, F.K. and Redkopp, L.G., 1991. The stability of a sheared density interface. Phys. Fluids A, 3(10): 2360–2370.

Lindzen, R.S. and Rosenthal, J., 1976. On the instability of Helmholtz velocity profiles in stably stratified fluids when a lower boundary is present. J. Geophys. Res., 81: 1561–1571.

Murota, A. and Hirata, K., 1978. Properties of internal waves and mixing mechanisms on density stratified flows. Proc. 22nd Symp. Hydraulics, JSCE, pp. 107–112 (in Japanese).

Nishida, S. and Yoshida, S., 1987. Stability and eigenfunctions of disturbances in stratified two-layer shear flow. Proc. 3rd Int. Symp. on Stratified Flows, Pasadena, CA. ASCE, AGU, pp. 28–34.

Sargent, F.E. and Jirka, G.H., 1987. Experiments on saline wedge. J. Hydraul. Eng., 113(10): 1307–1324.

Tsubaki, T., Hamamura, M. and Hashimoto, M., 1969. On the statistical properties of internal waves formed at the interface of arrested saline wedges. Proc. 13th Congress of IAHR, Kyoto. Science Council of Japan, C17: 63–74.

Yonemitsu, N., 1991. The stability and interfacial phenomena of a salt wedge flow. Ph.D. Thesis, University of Alberta, Edmonton.

Yoshida, S., 1980. Mixing mechanisms of density current system at a river mouth. 2nd Int. Symp. on Stratified Flows, Trondheim, Norway. IAHR, pp. 1062–1073.